Photocatalytic degradation of methylene blue dye in aqueous solution using $Bi_{(2-x)}M_xO_{(3-2.5x)}$:$Co_3O_4$ semiconductor catalyst

Niyazi A. S. Al-Areqi[1], Elyas S. Al-Aghbari[1] , Waddhaah M. Al–asbahy[1], Dina M.Murshed[1,*], Fuad Saleh[2]

Abstract—The present study involves the photocatalytic degradation of methylene blue in aqueous solution by $Bi_{(2-x)}M_xO_{(3-2.5x)}$: Co_3O_4 semiconductor catalyst. that the variation of band-gap energy with Cu content (x) shows a minimum (E_g~1.807eV) at x=0.05,wich is significantly lower than E_g value of Co_3O_4 .However, the unexpected increase of Eg for x= 0.02 and x=0.08 may be attributed to scattering of UV-VIS radiation beam which is incident on the sample during the measurements as a result of high crystallinity of these two compositions. E_g shows otherwise a general increase with increasing Ni content (*x*). This indicates that the crystallinity increases with the partial substitution of Ni for Bi in the lattice positions. This might be the reason behind the scattering of incident UV-VIS beam during the spectral measurements. The value of E_g goes on decreasing remarkably with the increase of Cr- content , reaching a minimum (E_g~ 1.7171eV) for *x*=0.05, and there after it is raised up. This minimum E_g value observed for Cr- system is more significantly lower than that of Co_3O_4 as compared with the minimum Eg value of Cu- system at the same doping level. Almost, the linearity of kinetic profiles can be seen, except for Ni-doped Bi_2O_3, where deviations from the linearity are observed at high irradiation times, particularly with higher Ni-dopant concentrations. This actually presumes a kinetic order that is greater than the unity (i-e, n>1) for the photocatalytic degradation in the presence of Ni-doped Bi_2O_3:Co_3O_4. The photocatalytic degradation of MB in the presence of undipped Bi_2O_3:Co_3O_4(K_{app}~0.0093 min^{-1}) is nearly two orders of magnitude faster than that in the presence of the only Co_3O_4 semiconductor (K_{app}~ 0.00198 min^{-1}). The Cu-doped Bi_2O_3 shows a maximum photocatalytic efficiency (k_{app} ~ 0.089 min^{-1}) for the composition *x*=0.02, and beyond this it sharply drops by many orders of magnitude , as compared to undoped Bi_2O_3:Co_3O_4 and the only Co_3O_4 as well . On other hand, the photocatalytic efficiency of Ni-doped Bi_2O_3:Co_3O_4 composites drastically increases as Ni content increases.

Keywords: Band-gap energy , blue , catalyst , degradation , methylene, photocatalytic, semiconductor.

1 INTRODUCTION

SYNTHETIC dyes comprise an important part of industrial water effluents, discharged in abundance by many manufacturing industries. The impact of such dyes on the environment is a major concern, because of their potentially carcinogenic properties. Besides this, some dyes can undergo anaerobic discoloration to form potential carcinogens [1-2].

Various physico-chemical techniques are available for the elimination of dyes from wastewater and in particular photocatalysis is a more promising tool. Moreover, photocatalysis can be used to cause redox transformations and decompose a dye molecule. The use of photosensitive semiconductors such as TiO_2, ZnO, Fe_2O_3, CdS, ZnS and V_2O_5 has been reported in the literature for their use in reducing color of the dye solutions owing to their environmental-friendly benefits in the saving of resources such as water, energy, chemicals, and other cleaning materials. This is mainly because of its various merits, such as Titanium dioxide (TiO_2) mediated based photodegradation has attracted extensive interest owing to its great advantages in the complete removal of organic pollutants from wastewater optical-electronic properties, low-cost, chemical stability, and nontoxicity [3-7]. Azo dyes are the largest group of synthetic colorants (60–70 %) and are being used in industry for applications such as textiles, papers, leathers, gasoline, additives, foodstuffs, cosmetics, laser materials, xerography, laser printing, etc. and the resulted by-products contain both dyes and metal ions. Methylene Blue (methylthionine chloride) is a heterocyclic aromatic chemical compound with molecular formula ($C_{16}H_{18}ClN_3S$, $_3H_2O$) **(**Figure 1**)** with the chemical name [3, 7-bis (dimethyl amino) phenazathionium chloride tetra methylthionine chloride] [8,9]. Methylene blue (MB) is a cationic thiazine dye that is deep blue in the oxidized state while it is colorless in its reduced form (leucomethylene blue). MB and leucomethylene blue exist as a redox couple in equilibrium and together form a reversible oxidation-reduction system or electron donor acceptor couple. [10].

Among many known Advanced oxidation process (AOPs), photocatalytic degradation has proven to be a remising technology for degrading organic compounds. The technique is more effective as compared to other AOPs because semiconductors are inexpensive and can easily mineralize various organic compounds. the basic steps of heterogeneous photocatalysis consist of initially transferring of the reactants in the liquid phase ontothe liquid phase.

- [1]*Department of Chemistry. Faculty of Applied Science, Taiz University, Taiz, Yemen. * Corresponding Author E-mail: dinaalquobaty2018@gmail.com (Dina M.Murshed).*
- [2]*Department of Industrial Chemistry. Faculty of Applied Science, Taiz University, Taiz, Yemen.*

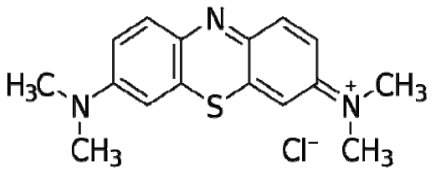

Fig.1. Chemical structure of methylene blue(MB).

The photocatalytic degradation of an organic compound such as dye is believed to take place according to the following mechanisms: when a catalyst is exposed to UV radiation, electrons are promoted from the valence band to the conduction band. As a result of this, an electron–hole pair is produced.

$$\text{Catalyst} + h\nu \rightarrow e^{-}_{cb} + h^{+}_{vb} \qquad (1)$$

where, e^{-}_{cb} and h^{+}_{vb} are the electrons in the conduction band and the electron vacancy in the valence band, respectively. Both these entities can migrate to the catalyst surface, where they can enter in a redox reaction with other species present the catalyst surface followed by adsorption of the reactant on the catalyst surface, reaction in the adsorbed phase, desorption of the final product and finally removal of the final products in on the surface. In most cases h^{+}_{vb} can react easily with surface bound H_2O to produce $OH^{\bullet}$ radicals, whereas, ecb can react with O_2 to produce superoxide radical anion of oxygen.

$$H_2O + h^{+}_{vb} \rightarrow OH^{-} + H^{+} \qquad (2)$$

$$O_2 + e^{-}_{cb} \rightarrow O^{-}_{2} \qquad (3)$$

this reaction prevents the combination of the electron and the hole which are produced in the first step. The $OH^{\bullet}$ and O^{-2} produced in the above manner can then react with the dye to form other species and is thus responsible for the discoloration of the dye.

$$O_2 + H^{+} \rightarrow HO^{-}_{2} \qquad (4)$$

$$H_2O_2 \rightarrow 2OH^{\cdot} \rightarrow 2OH^{\cdot} \qquad (5)$$

$$OH^{\cdot} + dye \rightarrow dye(k = 10^{9} - 10^{10} M^{-1}S^{-1}) \qquad (6)$$

$$Dye + e^{-}_{cb} \rightarrow reduction\ product \qquad (7)$$

It may be noted that all these reactions in photocatalysis are possible due to the presence of both dissolved oxygen and water molecules. Without the presence of water molecules, the highly reactive hydroxyl radicals ($OH^{\bullet}$) could not be formed and inhibit the photodegradation of liquid phase organic molecules.

The present research work has been devoted to achieve the following objectives:

(i) Solving one of the important of environmental and health problem relating to pollution of water with synthetic dyes.

(ii) To develop a new semiconducting photocatalyst as a bina ry oxides; pure Co_3O_4 and M-doped Bi_2O_3 (M= Cu^{2+}, Cr^{3+}, and Ni^{2+}), prepared by citrate-ethylene glycol sol-gel method.

(iii) To investigate the photocatalytic efficiency of prepared semiconducting binary system on the degradation of MB dye in aqueous solutions under visible-light irradiation.

2 Materials & Methods

2.1 Preparations of photocatalyst

2.1.1 Preparation of Co_3O_4

Co_3O_4 was prepared using sol-gel route by mixing accurately amounts of $(CH_3COO)_2Co.4H_2O$ solution (0.10 M) with chelating agent consisting of an 1:4 mixture of citric acid (0.3 M) and ethylene glycol (0.5M). The resulting sol was thoroughly mixed together. Thereafter, NH_3 solution was added which heated at 80-90 C° with continuous stirring. The resulting xerogel was dried and then claimed in a muffle furnace at 500 ºC for 12 hours. After complete calcination, the oxide produced was allowed to slowly quench in air to room temperature.

2.1.2 Preparation of $Bi_{(2-x)}M_xO_{(3-2.5x)}$

$Bi_{(2-x)}M_xO_{(3-2.5x)}$;(M=Ni^{2+}, Cr^{3+}, Cu^{2+}) in composition range $0 \le x \le 0.08$ was prepared using sol-gel route by mixing accurately amounts of 0.1M $Bi(NO_3)_3$ solution and $Ni(CH_3COO)_2.4H_2O$ solution (0.10 M) with chelating agent consisting of an 1:4 mixture of citric acid, CA (0.3 M) and ethylene glycol, EG (0.5 M) as shown in Table 1. The resulting sol was thoroughly mixed together. Thereafter, NH_3 solution was added which heated at 80-90 °C with continuous stirring. The resulting xerogel was dried and then calcaned in a muffle furnace at 500 °C for 12 hours. After complete calcination, the oxide produced was allowed to slowly quench in air to room temperature.

TABLE 1
DIFFERENT COMPOSITIONS OF $Bi_{(2-x)}M_xO_{(3-2.5x)}$ PREPARED BY SOL-GEL ETHYLENE GLYCOL -CITRATE ROUTE.

x	*mg* $Bi(NO_3)_3$	*mL* $Ni(CH_3COO)_2$ *or mL* $Cu(CH_3COO)_2$ *or mL* $Cr(CH_3COO)_3$	*mL CA/EG*
0	3.949	0	50
0.02	2.843	10	50
0.05	1.482	25	50
0.08	0.474	40	50

2.3 Preparation of MB dye solution

Accurately weighed amount of methylene blue (MB) dye ($C_{16}H_{18}ClN_3S$, MW=319.85 g/mol) was dissolved in distilled water to obtain an aqueous dye solution with an exact concentration of 1.0 ×10^{-5} M.

2.4 Optical properties of photocatalysts

A thin layer of photocatalyst oxide was painted on a clean glass strip with the help of water. After drying, UV-VIS spectra for all photocatalysts investigated were recorded using a UV-VIS Spectrophotometer (schimatzu 2450) in the wavelength range 250 -780 nm. The band- gap energies (E_g) were then calculated using the relation:

$$E_g\ (eV) = 1244.25/\lambda_g\ (nm) \qquad (8)$$

where λ_g(nm) is the wavelength of absorption edge expressed in nanometers.

2.5 UV-Visible spectrum of MB dye

UV-VIS spectrum of MB dye aqueous solution (1.1×10^{-5} M) was recorded by scanning in the range of 250-780 nm using a UV-VIS Spectrophotometer (schimatzu 2450).

2.6 Adsorption experiments

Adsorption capacity (Q_{max}) and specific surface area (S) of photocatalyst samples were determined using MB adsorption on to photocatalyst sample in aqueous solution. Accurately weighed amount of a photocatalyst was added in to 10ml MB aqueous solution (1.5×10^{-5} M). The mixture was shaked vigorously for 1hour and was then left on standing in the dark place for 24 hours to acquire an adsorption equilibrium. Approximately 5ml of the mixture was centrifuged at intermediate speed and absorbance of supernatant (A_r) was measured at λ= 660 nm using a schimatzu UV-VIS spectrophotometer (UV-2450). According to the Langmuir adsorption isotherm, Q_{max} and S were calculated using the following relations, respectively:

$$Q_{max}\ (mgg^{-1}) = (C_o \times V \times MW(D) \times (1-A_r/A_o))/WZ \qquad (9)$$

$$S(m^{-2}g^{-1}) = (656.48 \times V \times C_o \times A_r)/(WZ \times A_o) \qquad (10)$$

where C_o is the initial concentration of MB solution (1.5×10^{-5} M), V is the volume of MB solution used for the a desorption, MW(D) is the molecular weight of MB (319.85), W_Z is the weight of photocatalyst sample added (expressed in grams), and A_o, and A_r are the absorbance measured at 660 nm before and after adsorption, respectively. The calculation of S was based on considering the covered monolayer area of MB is equal to 1.08 nm^2/molecule [11].

2.7. Photocatalytic degradation experiments of MB dye

A 250 ml of 1.0×10^{-5} M dye solution was transferred into a 600 ml container photoreactor equipped with water refrigeration and magnetic stirrer. Accurately weighed 100 mg of the $Bi_{(2-x)}M_xO_{(3-2.5x)}$ and 100 mg of Co_3O_4 were dispersed in the dye solution. The resulting suspension was then magnetically stirred in the dark for 15 min to reach the adsorption–desorption equilibrium. A 300-W xenon lamp, located beyond an optical glass cut-off filter was used as the visible light source with wavelengths greater than 400 nm.

The irradiation source was located at 25 cm above the surface of liquid in the photoreactor. The temperature of reaction system was kept at 25 °C using flowing cool water in order to prevent the thermal catalytic reaction effect.

At equal time intervals of irradiation (10 min), 5 ml aliquot of the reaction mixture was withdrawn from the photoreactor and filtered to separate the catalyst residues. The dye concentration versus irradiation time (t) was determined by measuring the maximum absorbance at 660 nm using a Shimadzu UV–VIS spectrophotometer (UV-2450). The apparent rate constant (k_{app}) was computed using a pseudo first-order kinetic model according to Eqn (11):

$$\ln(A_t/A_o) = -k_{app}\,t \qquad (11)$$

Where A_t and A_o are the measured absorbance at time =t and at the initial time (t=0), respectively.

Experimental data were represented and analyzed using an Origin Pro.6.1.v6.1052 (B232), Origin Lab Corporation, *http://www.OriginLab.com.*

3 Results & Discussion

3.1 Optical properties of $Bi_{(2-x)}M_XO_{(3-2.5X)}$:$Co_3O_4$ series

UV-VIS absorption spectra of $Bi_{(2-x)}Cu_xO_{(3-2.5X)}$; $0.02 \leq x \geq 0.08$ and of Co_3O_4 are shown in Fig 2. The red lines represent the linear regression fitting to the spectral data in the region of absorption edges. The linear equations obtained from the fitted data have the form,

$$A = a - b\lambda \qquad (12)$$

where A is the value of absorbance measured at the wavelength (λ). A and B are the intercept and slope, respectively, when A is set zero, λ_g=λ. Table 2 summarizes the estimated values of λ_g and band-gap energy for $Bi_{(2-x)}Cu_xO_{(3-2.5X)}$ and Co_3O_4 along with their statistical parameters. It is clearly observed that the variation of band-gap energy with Cu content (x) shows a minimum (E_g~1.807ev) at x=0.05,wich is significantly lower than Eg value of Co_3O_4 .However, the unexpected increase of E_g for x= 0.02 and x=0.08 may be attributed to scattering of UV-VIS radiation beam which is incident on the sample during the measurements as a result of high crystallinity of these two compositions in the similar manner to what have been reported for other Bi- containing oxides [12] using absorption mode of spectral measurements.

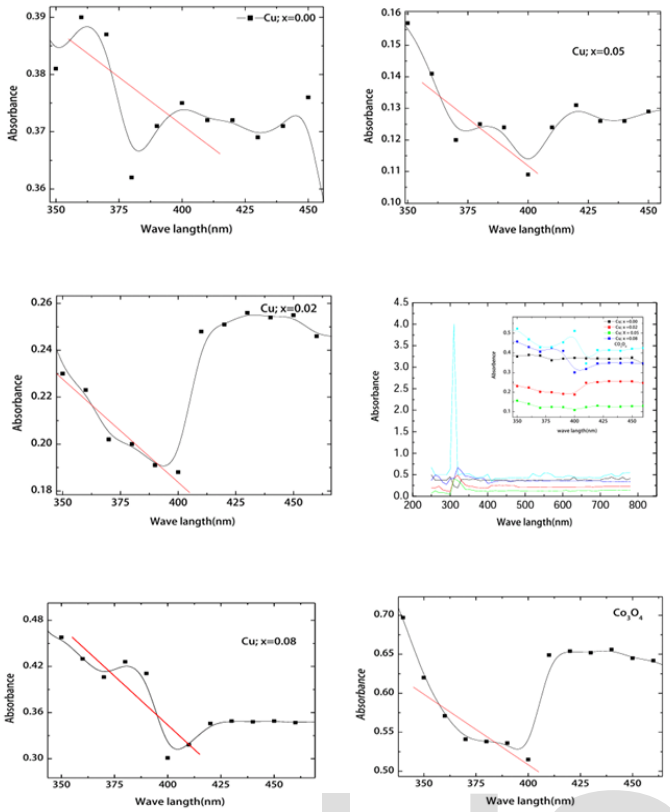

Fig.2. UV-VIS absorption spectra of $Bi_{(2-x)}Cu_xO_{(3-2.5)}$; 0.02≤ x ≥ 0.08 and of Co_3O_4The red lines represent the linear regression fitting to the spectral data in the region of absorption edges.

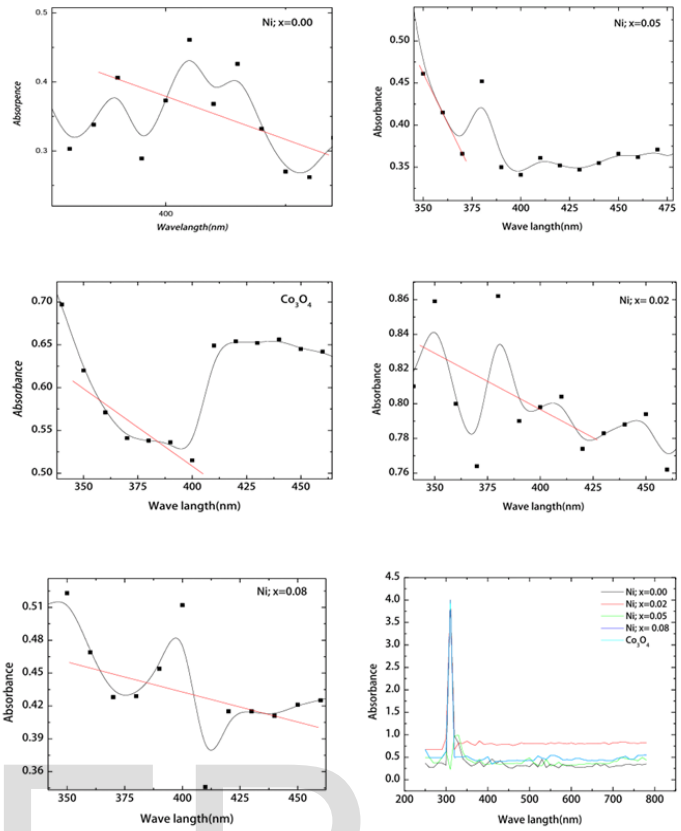

Fig.3. UV-VIS absorption spectra of $Bi_{(2-x)}Ni_xO_{(3-2.5)}$; 0.02≤ x ≥ 0.08 and of Co_3O_4.

TABLE 2
BAND-GAP ENERGIES OF $Bi_{(2-x)}Cu_xO_{(3-2.5x}$ AND Co_3O_4 WITH THEIR STATISTICAL PARAMETERS.

Composition	λ_g*(nm)*	E_g*(eV)*	R^2	*SD*
Bi_2O_3	658.982	1.912	0.8323	0.0371
$Bi_{1.98}Ni_{0.02}O_{2.99}$	639.506	1.970	1	0.0192
$Bi_{1.95}Ni_{0.05}O_{2.975}$	549.066	2.951	0.9564	0.0250
$Bi_{1.92}Ni_{0.08}O_{2.96}$	416.207	3.027	0.8623	0.0200
Co_3O_4	651.779	1.933	0.8835	0.0120

TABLE 3
BAND-GAP ENERGIES OF $Bi_{(2-x)}Ni_xO_{(3-2.5x)}$ AND Co_3O_4 WITH THEIR STATISTICAL PARAMETERS.

Composition	λ_g*(nm)*	E_g*(eV)*	R^2	*SD*
Bi_2O_3	574.141	2.195	0.6150	0.0151
$Bi_{1.98}Cu_{0.02}O_{2.99}$	542.121	2.324	0.8418	0.0082
$Bi_{1.95}Cu_{0.05}O_{2.975}$	697.399	1.807	0.0051	0.0026
$Bi_{1.92}Cu_{0.08}O_{2.96}$	526.123	2.395	0.4072	0.0025
Co_3O_4	651.779	1.933	0.8835	0.0117

Fig.3 presents UV-VIS absorption spectra of $Bi_{(2-x)}Ni_xO_{(3-2.5)}$; $0.02 \le x \ge 0.08$, and of Co_3O_4. The estimated values of λ_g and E_g and corresponding statistical parameters are listed in Table 3. It is interesting to note that the E_g shows otherwise a general increase with increasing Ni content (x).

This indicates that the crystallinity increases with the partial substitution of Ni for Bi in the lattice positions. This might be the reason behind the scattering of incident UV-VIS beam during the spectral measurements [12].

Similarly, Fig.4. and Table 4. show the UV-VIS spectra and estimated values of λ_g and E_g, respectively, of $Bi_{(2-x)}Cr_xO_{(3-3x)}$; $0.02 \le x \ge 0.08$ and Co_3O_4.The important point to be emphasized here is that the value of Eg goes on decreasing remarkably with the increase of Cr- content , reaching a minimum (E_g ~ 1.7171ev) for x=0.05, and there after it is raised up. This minimum E_g value observed for Cr- system is more significantly lower than that of Co_3O_4 as compared with the minimum E_g value of Cu- system at the same doping level.

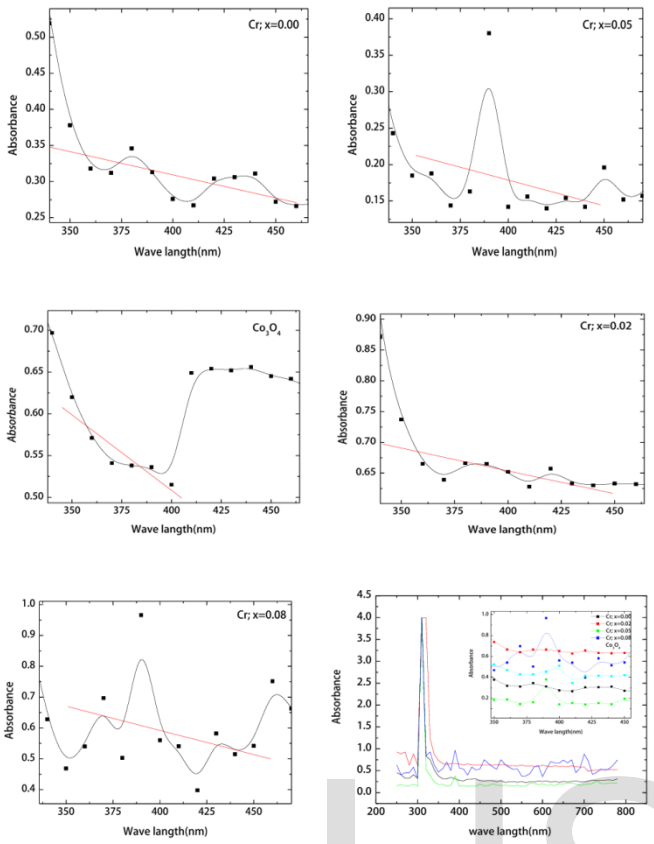

Fig.4. UV-VIS spectra and estimated values of λg and E_g, respectively, of $Bi_{(2-x)}Cr_xO_{(3-3x)}$; 0.02≤ x ≥ 0.08 and Co_3O_4.

TABLE 4
BAND-GAP ENERGIES OF $Bi_{(2-x)}Cr_xO_{(3-3x)}$ AND Co_3O_4 WITH THEIR STATISTICAL PARAMETERS.

Composition	λ_g*(nm)*	E_g*(eV)*	R^2	*SD*
Bi_2O_3	593.353	2.7302	0.3205	0.0134
$Bi_{1.98}Cr_{0.02}O_{2.94}$	582.681	2.1624	0.4455	0.0838
$Bi_{1.95}Cr_{0.05}O_{2.85}$	733.415	1.7171	0.6141	0.0126
$Bi_{1.92}Cr_{0.08}O_{2.76}$	620.031	2.0322	0.9047	0.0436
Co_3O_4	651.779	1.9332	0.8835	0.0117

3.2 Adsorption efficiency of $Bi_{(2-x)}M_xO_{(3-3x)}$: Co_3O_4 series

MB dye was used in this research work, as it has been found to be extensively, commonly used standard dye in the researches related to the adsorption [11], and photocatalysis [12] investigations. Fig.5 depicts the UV-VIS spectrum of MB dye aqueous solution (1×10^{-5} M). A strong fundamental peak is observed at λ_{max}=660 nm, which is in a good agreement with its literature value reported [8]. However, at this maximum absorption wavelength, the absorbance of MB aqueous solution were measured in both adsorption and photocatalysis experiments. The estimated values of maximum adsorption capacity (Q_{max}) and the specific surface area (S) of $Bi_{(2-x)}Cu_xO_{(3-2.5x)}$ photocatalyst series based on MB adsorption equilibrium are summarized in Table 5.

It can be noted that the increase of S with Cu content is accompanied with a rise in the maximum MB loading at equilibrium adsorption (Q_{max}).

Similarly, the surface area of $Bi_{(2-x)}Ni_xO_{(3-2.5x)}$ goes on increasing with Ni content, except for x=0.02 (Table 6). Here in contrast, the increase of S is accompanied with a lowering in Q_{max}. Moreover, quite different mode in the variation of S and Q_{max} can also be observed for $Bi_{(2-x)}Cr_xO_{(3-3x)}$ series; as the increase of Cr content leads to decreased S and increased Q_{max}, except for x=0.08, where maximum Sand minimum Q_{max} are seen in Table 7. This indicates that there is no well-defined trend in the variation of S and Q_{max} as a function of a dopant concentration. However, it can be concluded that S generally increases in the order Cr> Ni>Cu, while Q_{max} shows a general increase in the order: Cu>Ni>Cr.

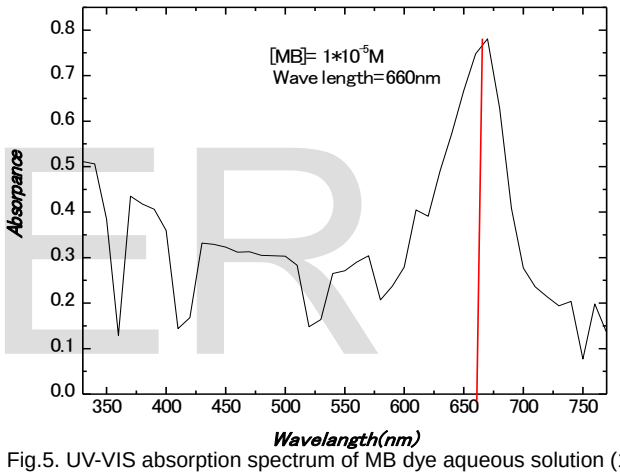

Fig.5. UV-VIS absorption spectrum of MB dye aqueous solution (1×10^{-5} M).

TABLE 5
ADSORPTION CAPACITIES AND SPECIFIC SURFACE AREAS OF $Bi_{(2-x)}Cu_xO_{(3-2.5x)}$ PHOTOCATALYST SERIES BASED ON MB.

Composition	Q_{max}*(mg.g^{-1})*	*S($m^2.g^{-1}$)*
Co_3O_4:Bi_2O_3	235.89	5.66×10^{-4}
Co_3O_4:$Bi_{1.98}Cu_{0.02}O_{2.95}$	221.22	5.36×10^{-4}
Co_3O_4:$Bi_{1.95}Cu_{0.05}O_{2.875}$	358.47	8.179×10^{-4}
Co_3O_4:$Bi_{1.92}Cu_{0.08}O_{2.8}$	2073.66	4.34×10^{-3}

TABLE 6
ADSORPTION CAPACITIES AND SPECIFIC SURFACE AREAS OF $Bi_{(2-x)}Ni_xO_{(3-2.5x)}$ PHOTOCATALYST SERIES BASED ON MB.

Composition	$Q_{max}(mg.g^{-1})$	$S(m^2.g^{-1})$
Co_3O_4:Bi_2O_3	36.80	6.53
Co_3O_4:$Bi_{1.98}Ni_{0.02}O_{2.95}$	38.35	3.34
Co_3O_4:$Bi_{1.95}Ni_{0.05}O_{2.875}$	3.38	12.65
Co_3O_4:$Bi_{1.92}Ni_{0.08}O_{2.8}$	32.91	14.52

TABLE 7
ADSORPTION CAPACITIES AND SPECIFIC SURFACE AREAS OF $Bi_{(2-x)}Cr_xO_{(3-3x)}$ PHOTOCATALYST SERIES BASED ON MB.

Composition	$Q_{max}(mg.g^{-1})$	$S(m^2.g^{-1})$
Co_3O_4:Bi_2O_3	20.73	39.51
Co_3O_4:$Bi_{1.98}Cr_{0.02}O_{2.94}$	32.66	14.82
Co_3O_4:$Bi_{1.95}Cr_{0.05}O_{2.85}$	38.10	3.74
Co_3O_4:$Bi_{1.92}Cr_{0.08}O_{2.76}$	1.87	85.90

3.3 Photocatalytic efficiency of $Bi_{(2-x)}M_xO_{(3-2.5x)}$:$Co_3O_4$ series

The photocatalytic efficiency of $Bi_{(2-x)}M_xO_{(3-2.5x)}$:Co_3O_4 binary oxides can be evaluated from the values of appear rent rate constant obtained by applying the pseudo-frist-0rder kinetic model to the experimental data of photocatalytic degradation of MB [19]. Figs 6 to 8 illustrate the kinetic profiles for the photocatalytic degradation of MB aqueous solution under visible-light irradiation with the addition of accurately weighed constant amount of the binary oxides; Cu- doped Bi_2O_3:Co_3O_4, Ni-doped Bi_2O_3: Co_3O_4, and Cr-doped Bi_2O_3:Co_3O_4, respectively. Almost, the linearity of kinetic profiles can be seen, except for Ni-doped Bi_2O_3, where deviations from the linearity are observed at high irradiation times, particularly with higher Ni-dopant concentrations. This actually presumes a kinetic order that is greater than the unity (*i.e.*, n >1) for the photocatalytic degradation in the presence of Ni-doped Bi_2O_3: Co_3O_4.

Estimated values of k_{app} obtained from corresponding profile slopes along with relevant statistical parameters for three photocatalyst systems are respectively listed in Tables 8 to 10. It can clearly be noticed that the photocatalytic degradation of MB in the presence of undipped Bi_2O_3:Co_3O_4(k_{app} ~ 0.0093 min^{-1}) is nearly two orders of magnitude faster than that in the presence of the only Co_3O_4 semiconductor (k_{app} ~ 0.00198 min^{-1}).

This suggests a charge-transfer mechanism/an acceptor-donor photosensitization mechanism [13] between Bi_2O_3 and Co_3O_4, *i.e.*, the excited photoelectrons are transferred from the conduction band of the donor Co_3O_4 to the conduction band of the acceptor Bi_2O_3.

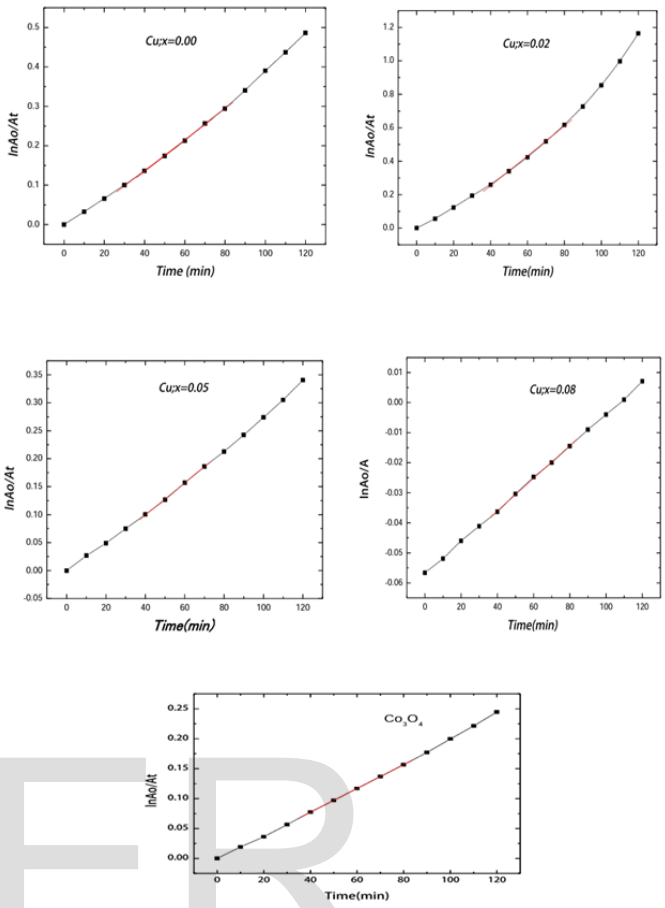

Fig.6. Pseudo first- order kinetic models for photocatalytic degradation of MB dye in the presence of $Bi_{(2-x)}Cu_xO_{(3-2.5x)}$:$Co_3O_4$ under visible- light irradiation.

The Cu- doped Bi_2O_3 shows a maximum photocatalytic efficiency (k_{app} ~ 0.089 min^{-1}) for the composition x=0.02, and beyond this it sharply drops (Table 8). by many orders of magnitude , as compared to undoped Bi_2O_3: Co_3O_4 and the only Co_3O_4 as well.

TAB LE 8
KINETIC PARAMETERS DEDUCED FROM THE PHOTOCATALYTIC DEGRADATION OF MB IN THE PRESENCE OF $Bi_{(2-x)}Cu_xO_{(3-2.5x)}$:$Co_3O_4$ UNDER VISIBLE-LIGHT IRRADIATION.

Composition	k_{app} (min^{-1})	R^2	*SD*
Co_3O_4:Bi_2O_3	0.0039	0.9853	0.00272
Co_3O_4:$Bi_{1.98}Cu_{0.02}O_{2.95}$	0.0089	0.9981	0.00719
Co_3O_4:$Bi_{1.95}Cu_{0.05}O_{2.875}$	-7.1429×10^{-6}	0.0051	0.00264
Co_3O_4:$Bi_{1.92}Cu_{0.08}O_{2.8}$	5.4161×10^{-4}	0.9987	3.50499×10^{-4}
Co_3O_4	0.00198	0.9999	2.14844×10^{-4}

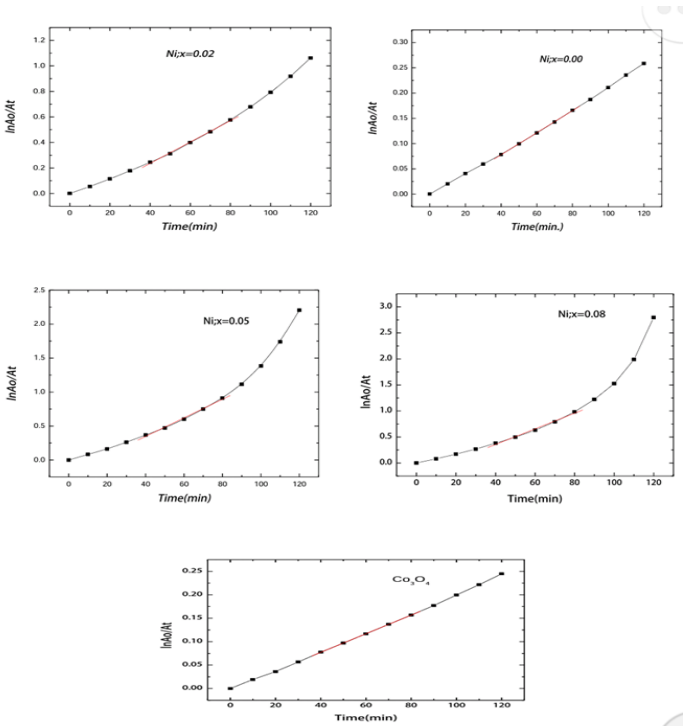

Fig 7. Pseudo first- order kinetic models for photocatalytic degradation of MB dye in the presence of $Bi_{(2-x)}Ni_xO_{(3-2.5x)}$:$Co_3O_4$ under visible- light irradiation.

On other hand, the photocatalytic efficiency of Ni- doped Bi_2O_3: Co_3O_4 composites drastically increases as Ni content increases (Table 9). Interestingly, the Ni- doped Bi_2O_3 shows more enhanced efficiencies for compositions with x= 0.05 and x= 0.08, It is worthwhile to point that the increase of photocatalytic efficiency for Ni- doped Bi_2O_3 series with the otherwise increase in E_g as a function of Ni content was also been seen with some other Ni- substituted oxides , such as Ni-doped $Bi_2VO_{5.5}$ [14, 15].

Now, combining the results of optical and adsorption characteristics, it is clear that the photocatalytic degradation of MB under visible-light irradiation in the presence of Ni-doped Bi_2O_3:Co_3O_4 composites is likely independent of the band –gap energy. As also seen from the adsorption efficiency of the Ni-doped Bi_2O_4 catalyst series having intermediate S and Q_{mas} values, it can be suggested that the rate-determining step of the photocatalytic degradation of MB proceeds at the surface of a photocatalyst. Since the photocatalysis of Ni-doped Bi_2O_4 has already been explored to be of on order greater than the unity (n >1), it is without a doubt that the rate of Ni- doped Bi_2O_3 photocatalysis is dependent on both MB and surface defect concentrations. Therefore, the rate law can be expressed as,

$$rate = k[MB][D]^m \qquad (13)$$

where, [MB] and [D] are the molar concentration of MB solution and surface defects of Ni-doped Bi_2O_3, respectively, m is the order of reaction with respect to the catalyst surface defects. The value of m may vary from 1/2 to 1. k is the theoretical rate constant, so that $k \leq k_{app}$. As surface defect concentration ([D]) is determined by the Ni dopant concentration ($[Ni^{+2}]$), it is convenient to get to get [D] equivalent to $[Ni^{+2}]$, and hence Eqn (13) simplifies to,

$$rate = k[MB][Ni^{+2}]^m \qquad (14)$$

Accordingly, the photocatalytic degradation of MB dye in the presence of Ni- doped Bi_2O_3:Co_3O_4 composites follows the (1+m) th-order kinetics *i.e.*, n may range from 3/2 to 2.

TABLE 9
KINETIC PARAMETERS DEDUCED FROM THE PHOTOCATALYTIC DEGRADATION OF MB IN THE PRESENCE OF $Bi_{(2-x)}Ni_xO_{(3-2.5x)}$: Co_3O_4 UNDER VISIBLE-LIGHT IRRADIATION.

Composition	k_{app} *(min^{-1})*	R^2	*SD*
Co_3O_4:Bi_2O_3	0.0039	0.99976	6.2878×10^{-4}
Co_3O_4:$Bi_{1.98}Ni_{0.02}O_{2.95}$	0.00837	0.99732	0.00791
Co_3O_4:$Bi_{1.95}Ni_{0.05}O_{2.875}$	0.01367	0.99313	0.02073
Co_3O_4:$Bi_{1.92}Ni_{0.08}O_{2.8}$	0.01504	0.990304	0.02715
Co_3O_4	0.00198	0.99996	2.14844×10^{-4}

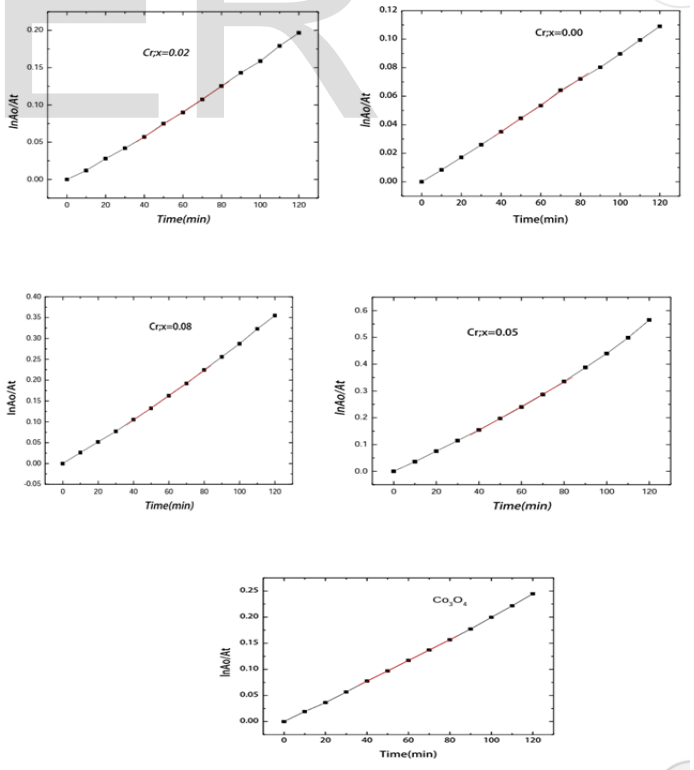

Fig.8. Pseudo first- order kinetic models for photocatalytic degradation of MB dye in the presence of $Bi_{(2-x)}Cr_xO_{(3-3x)}$:Co_3O_4 under visible- light irradiation

TABLE 10

KINETIC PARAMETERS DEDUCED FROM THE PHOTOCATALYTIC DEGRADATION OF MB IN THE PRESENCE OF $Bi_{(2-x)}Cr_xO_{(3-3x)}$: Co_3O_4 UNDER VISIBLE-LIGHT IRRADIATION.

Composition	k_{app} (min^{-1})	R^2	*SD*
Co_3O_4:Bi_2O_3	0.0039	0.99862	6.35646×10^{-4}
Co_3O_4:$Bi_{1.98}Cr_{0.02}O_{2.95}$	0.00169	0.99904	9.5344×10^{-4}
Co_3O_4:$Bi_{1.95}Cr_{0.05}O_{2.875}$	0.0045	0.99892	0.00269
Co_3O_4:$Bi_{1.92}Cr_{0.08}O_{2.8}$	0.00298	0.99898	0.00174
Co_3O_4	0.00198	0.99996	2.14844×10^{-4}

4 CONCLUSION

Recently, photocatalytic degradation has attained much more attention as a powerful purification technique for removal of organic pollutants, particularly, industrial dyes from wastewater.

In this research project, new attempts have been made for the development of photocatalysts based on binary semiconductor oxides, viz, $Bi_{(2-x)}M_xO_{(3-2.5X)}$:$Co_3O_4$; where M=$Cu^{+2}$,$Ni^{+2}$,and Cr^{+3} with the compositions range $0.02 \le x \le 0.08$. The optical properties of synthesized photocatalysts were investigated using UV-VIS absorpation spectrophtomatery. The adsorption of MB dye was utilized to determine the maximum adsorption capacity and to estimate the specific surface area of the photocatalyst series. Aqueous solution of MB dye were also used to investigate the photocatalytic effeciency of as-synthesized photocatalysts under visible-light irradiation. The relevant results showed that such binary-oxide photocatalysts work out via the charge-transfer mechanism between donor Co_3O_4 and acceptor M-doped Bi_2O_3. It can concluded that some of compositions, particularly, for Ni-doped Bi_2O_3 and Cr-doped Bi_2O_3 can be employed as catalysts with more enhanced photocatalytic efficiency for the degradation of organic dyes and pollutants using visible light or sun light as a source of irradation. It was also found that the photocatalytic degradation of MB using Ni- doped Bi_2O_3:Co_3O_4 has a kinetic order greater than the unity, i.e., the rate of degradation is dependent on the Ni dopant concentration as well.

ACKNOWLEDGEMENTS

The authors would like to thank Prof. Helmi Alsheibani, Dean Faculty of Education, Taiz University and Dr. Hakim Q. N M. Al-Areque, Chairman of Department of Chemistry, Faculty of Education, Taiz University, Temen for providing research facilities.

REFERENCES

[1] M. Zubair Alam, S. Ahmad, A. Malik, M. Ahmad, Mutagenicity and genotoxicity of tannery effluents used for irrigation at Kanpur, India, *Ecotoxicology and Environmental Safety* 73(2010) 1620-1628.

[2] M. E. Pérez, D. M. Ruiz, M. Schneider, J. C. Autino and G. Romanelli, "La química verde como fuente de nuevos compuestos para el control de plagas agrícolas". Revista Ciencia en Desarrollo, vol, 4 no. 2, pp.83-91, 2013.

[3] F. H. AlHamedi, M.A. Rauf, S. S. Ashraf, Degradation studies of Rhodamine B in the presence of H_2O_2/ UV, *Desalination* 239 (2009) 159-166.

[4] M. R.. Hoffman, S. T. Martin, W. Choi, D. W. Bahnemann, Environmental Application of Semiconductor Photocatalysis.*Chem. Rev*. 1995, 95, 69–96.

[5] B.Li, X. Wang, M. Yan,; L. Li, Preparation and characterization of nano-TiO_2 powder.*Mater. Chem. Phys*.2002, 78, 184–188.

[6] J. C. Yu, J. G Yu, J. C. Zhao, Enhanced photocatalytic activity of mesoporous and ordinary TiO2thin films by sulfuric acid treatment. *Appl. Catal., B*, 36(2002)31–42.

[7] D. Vaya, V.K. Sharma, Study of synthesis and photocatalytic activities of Mo doped ZnO. *J. Chem. Pharm. Res.* 2(2010) 269-273.

[8] www.wikipedia.com/methylene blue.

[9] L.V. Jian-xiao, C. Ying, X. Guo-hong, Z. Ling-yun, W. Su-fen Decoloration of methylene blue simulated wastewater using a UV-H_2O_2 combined system. *Journal of Water Reuse and Desalination* 1(2011) 45-51.

[10] A.E.H.Machado, J.A.de Miranda, R.F.de Freitas,E.T.F.M.Duarte, L.F.Ferreira,Y.D.T.Albuquerque, R.Ruiggiero, C.Sattler,L. de Oliveira, Destruction of the organic matter present in effluent from a cellulose and paper industry using photocatalysis, *Journal of Photochemistry and Photobiology A:Chemistry* 155 (2003) 231-241.

[11] A.U. ltodo, and M.K. Gafar, Estimation of specific surface area using Langmuir isotherm method, *J.Appl. Sci. Environ. Manage.* 14 (4) (2010) 141-145.

[12] A.M.A. Alfatish, *Photocatalytic efficiency of Auttivillius-type layered BIMEVOXES for the photocatalytic degradation of organic dyes in aqueous media under visible-light irradiation*, M.Sc. Dissertation, Taiz Uni.,(2019).

[13] A.A.Abdullah, A.R.Dahoh, M.M.Ahmed, and N.M.Abdalgalil, *Photocatalytic degradation of MB dye in aqueous solution in the presence of semiconductor catalyst*, B.Sc. Grad. Res. Proj., Taiz uni., (2017)

[14] N.A.S. Al-Ariqi, A.S.N.Al-Kamali, Kh.A.S. Ghaleb, A. Al-Alas, K.Al-Mureish, Influence of phase stabilization and perovskite-vanadate oxygen vacancies of BINIVOX catalyst on photocatalytic degradation of azo dye under visible light irradiation, *Radiation Effect and Defects in Solids*, 169 (2014) 117-128.

[15] N.A.S. Al-Ariqi, A. Al-Alas, A.S.N. Al-Kamali, Kh.A.S. Ghaleb, K. Al-Mureish, Photodegradation of 4-SPPN dye catalyzed by Ni(ll)-substituted $Bi_2VO_{5.5}$ system under visible light irradiation: Influence of phase stability and perovskite vanadate-oxygen vacancies of photocatalyst, *Journal of Molecular Catalysis A: Chemical*, 381 (2014)1-8.